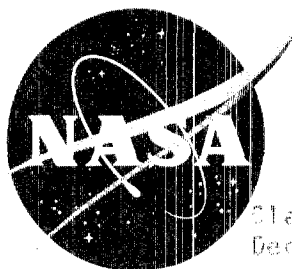Copy

NASA TM X-345

Classification Changed to
Declassified Effective 18 April
Authority NASA CCN-3 By J.J.Carr

TECHNICAL MEMORANDUM
X-345

A TRANSONIC WIND-TUNNEL INVESTIGATION

OF THE STATIC LONGITUDINAL AND LATERAL AERODYNAMIC

CHARACTERISTICS OF A PROPOSED HYPERSONIC GLIDER

WITH SEVERAL BOOSTER CONFIGURATIONS

By Ralph P. Bielat

Langley Research Center
Langley Field, Va.

NATIONAL AERONAUTICS AND SPACE ADMINISTRATION

WASHINGTON

December 1960

CONFIDENTIAL

NATIONAL AERONAUTICS AND SPACE ADMINISTRATION

TECHNICAL MEMORANDUM X-345

A TRANSONIC WIND-TUNNEL INVESTIGATION

OF THE STATIC LONGITUDINAL AND LATERAL AERODYNAMIC

CHARACTERISTICS OF A PROPOSED HYPERSONIC GLIDER

WITH SEVERAL BOOSTER CONFIGURATIONS*

By Ralph P. Bielat

SUMMARY

An investigation was conducted at transonic speeds in the Langley 8-foot transonic pressure tunnel to obtain the static longitudinal and lateral aerodynamic characteristics of a proposed hypersonic glider with several booster configurations. The Mach number range extended from 0.70 to 1.20, the angle of attack varied from approximately -6° to 8°, and the angle of sideslip varied from approximately -5° to 5°. The Reynolds number of the tests based on the glider wing mean aerodynamic chord ranged from approximately 1.08×10^6 to 1.89×10^6.

The results indicate that the only configurations which may have satisfactorily longitudinal stability characteristics were those with the horizontal booster fins and the only configurations which may have favorable directional stability characteristics were those with the interdigitated booster fins. Most of the configurations indicated negative effective dihedral as the Mach number was increased to 1.20.

INTRODUCTION

A research program has been carried out at the Langley Research Center to obtain aerodynamic data at transonic and supersonic speeds of a proposed hypersonic glider and booster configuration for the purpose of evaluating the glider-booster combination during a portion of the booster phase. As part of this program, basic pressure measurements on the boosters have been reported in reference 1. The present paper

---

*Title, Unclassified.

presents the results of wind-tunnel tests made in the Langley 8-foot transonic pressure tunnel on two booster configurations with the glider, on two booster-fin configurations with the glider, and on a booster-fin configuration with the glider removed and replaced with a conical-nose section. The tests were made at Mach numbers from 0.70 to 1.20 for angles of attack varying from -6° to 8° and for angles of sideslip varying from -5° to 5°. Additional tests with glider elevon deflections of 0° and ±15° were also made. The Reynolds number of the tests, based on the glider wing mean aerodynamic chord, ranged from approximately 1.08×10^6 to 1.89×10^6.

SYMBOLS

All aerodynamic data have been reduced to nondimensional coefficients. The data are referred to a set of axes coinciding with the booster body axes and originating in the model plane of symmetry at the trailing edge of the glider wing which corresponds to model station 10.638 inches.

A   booster base area, sq ft

b   glider wing span, ft

$\bar{c}$ glider wing mean aerodynamic chord, ft

C_A axial-force coefficient, $\dfrac{\text{Axial force}}{qS}$

$C_{A,b}$ base axial-force coefficient, $\dfrac{(p_b - p)A}{qS}$

$C_{A_{\alpha=0^\circ}}$ axial-force coefficient at $\alpha = 0^\circ$

C_l rolling-moment coefficient, $\dfrac{\text{Rolling moment}}{qSb}$

C_m pitching-moment coefficient, $\dfrac{\text{Pitching moment}}{qS\bar{c}}$

C_n yawing-moment coefficient, $\dfrac{\text{Yawing moment}}{qSb}$

C_N normal-force coefficient, $\dfrac{\text{Normal force}}{qS}$

C_Y side-force coefficient, $\dfrac{\text{Side force}}{qS}$

C_{l_β} rate of change of rolling-moment coefficient with sideslip angle measured at $\beta = \pm 1^\circ$, $\dfrac{\partial C_l}{\partial \beta}$, per deg

C_{m_α} pitching-moment-curve slope measured at $\alpha = \pm 1^\circ$, $\dfrac{\partial C_m}{\partial \alpha}$, per deg

C_{n_β} rate of change of yawing-moment coefficient with sideslip angle measured at $\beta = \pm 1^\circ$, $\dfrac{\partial C_n}{\partial \beta}$, per deg

C_{N_α} normal-force-curve slope measured at $\alpha = \pm 1^\circ$, $\dfrac{\partial C_N}{\partial \alpha}$, per deg

C_{Y_β} rate of change of side-force coefficient with sideslip angle measured at $\beta = \pm 1^\circ$, $\dfrac{\partial C_Y}{\partial \beta}$, per deg

$C_{m_{\delta_e}}$ elevon control effectiveness parameter measured at $\delta_e = \pm 1^\circ$, $\dfrac{\partial C_m}{\partial \delta_e}$, per deg

M free-stream Mach number

p free-stream static pressure, lb/sq ft

p_b base pressure, lb/sq ft

q free-stream dynamic pressure, lb/sq ft

R Reynolds number based on $\bar{c}$

r radius

S glider wing area, sq ft

α angle of attack, referred to booster center line, deg

β angle of sideslip, referred to plane of symmetry, deg

δ_e elevon deflection, positive when trailing edge is down, deg

Model Component Designations

B_1 first-stage advanced booster

B_2 second-stage advanced booster

B_{1T} first-stage original booster

B_{2T} second-stage original booster

F_1 horizontal booster fins in plane of glider

F_2 interdigitated booster fins

G   glider

N   conical nose

APPARATUS

Tunnel

The investigation was made in the Langley 8-foot transonic pressure tunnel. This facility is rectangular in cross section with the upper and lower walls slotted longitudinally to allow continuous operation through the transonic speed region with negligible effects of choking and blockage for the size models used in the present investigation. During the investigation the tunnel was operated at various values of stagnation pressures in order to maintain a constant value of Reynolds number through the Mach number range. The stagnation temperature and dewpoint were maintained at a level to preclude shock condensation effects.

Model

The models of the present investigation were 1/37-scale models of a proposed hypersonic glider-booster configuration and were constructed of stainless steel. Details of the models are given in figures 1 and 2.

The models included a glider, two booster configurations, two booster-fin configurations, and a conical nose which was interchangeable with the glider. The glider wing had leading-edge-sweep angles of 76° and 60° of the inboard and outboard panels, respectively, an aspect ratio of 1.032, and utilized a modified-wedge airfoil section parallel to the plane of symmetry. The wing incorporated elevons which could be deflected to ±15°. The vertical fins, which were located on the wing tips, had a leading-edge sweep of 40°, a taper ratio of 0.832, an aspect ratio of 1.045, and used a modified-wedge airfoil section. The two booster configurations were cylindrical in cross section and represent the first and second stages of an original booster and the first and second stages of an advanced booster. Two booster-fin configurations were tested, one of which had two fins located parallel to the plane of the glider wing and had a leading-edge sweep of 43.5°, a taper ratio of 0.462, an aspect ratio of 0.697, and used a modified-wedge airfoil section. The second fin configuration, which had four fins interdigitated with respect to the glider wing, had a leading-edge sweep of 45°, a taper ratio of 0.834, an aspect ratio of 0.181, and used a slab airfoil section. A photograph of the glider with the first and second stages of the original boosters is shown in figure 3.

TESTS

The wind-tunnel tests were made at Mach numbers from 0.70 to 1.20 for an angle-of-attack range of -6° to 8°, an angle-of-sideslip range from -5° to 5°, and for elevon deflections of 0° and ±15°. It was desired to maintain a constant Reynolds number of 3.5×10^6 per foot throughout the Mach number range; however, for certain configurations, it was necessary to reduce the Reynolds number to a value of 2.0×10^6 per foot in order not to exceed balance load limits. As a result, the Reynolds numbers of the tests, based on the glider wing mean aerodynamic chord, varied from 1.08×10^6 to 1.89×10^6. The Reynolds number for each configuration tested is given in the figures presenting the results.

All tests were conducted with fixed transition on the glider according to the methods described in reference 2. The strips were approximately 0.10 inch wide and were formed by sprinkling No. 120 carborundum grains on a plastic adhesive. The strips extended from the wing-body juncture to the wing tip at 0.25 inch measured perpendicular to the wing leading edge on the upper and lower wing surfaces. The transition strip was also carried around the body at the intersection of the strip at the wing-body juncture. A transition strip was also

applied on the conical-nose section approximately 2 inches back from the nose. Transition strips were not used on the booster fins.

MEASUREMENTS AND ACCURACY

Six-component data were obtained by means of an electrical strain-gage balance located inside the boosters. Static base pressures were measured and were used to adjust the drag data to free-stream conditions at the model bases. The base axial-force coefficients for several configurations are given in figure 4. No measurements were taken in the Mach number range where the data would be affected by reflected disturbances from the test-section boundary.

No corrections for the forces and moments produced by the sting interference have been applied to the data. As indicated in reference 3, the significant corrections would be limited to small increments in pitching moment and drag and to the effective downwash angle.

The angles of attack and sideslip have been corrected for deflection of the sting-support system under load and for flow angularity in the wind tunnel. The angles of attack, sideslip, and control deflection are estimated to be accurate to within $\pm 0.1^\circ$.

The estimated accuracy of the data at a Mach number of 0.90, based on the static calibrations, is as follows:

C_N . . . . ± 0.01

C_A . . . . ± 0.003

C_m . . . . ± 0.028

C_l . . . . ± 0.001

C_n . . . . ± 0.035

C_Y . . . . ± 0.01

RESULTS AND DISCUSSION

Longitudinal Aerodynamic Characteristics

The basic static longitudinal aerodynamic characteristics for the various model configurations are presented in figures 5 to 9 and the summary data are given in figures 10 and 11.

Normal-force characteristics.- The normal-force-curve slope C_{N_α} for the glider with original boosters was essentially the same as that for the glider with advanced boosters and both configurations showed little variation with Mach number (fig. 10). Adding the interdigitated booster fins $\left(F_2\right)$ to the glider with the original boosters increased the normal-force-curve slope approximately 37 percent over the Mach number range, whereas the normal-force-curve slope for the glider configuration with original boosters and horizontal booster fins $\left(GB_{2T}B_{1T}F_1\right)$ was about 2.0 to 2.5 times the values for the configuration without fins. The variation of normal-force-curve slope with Mach number was also more pronounced for the glider configuration with original boosters and horizontal booster fins than that for the configuration without fins. The normal-force-curve slope characteristics for the conical-nose configuration with original boosters and horizontal booster fins $\left(NB_{2T}B_{1T}F_1\right)$ were somewhat lower but similar to those of the glider configuration $\left(GB_{2T}B_{1T}F_1\right)$.

Axial-force characteristics.- A comparison of the axial-force coefficients measured at 0° angle of attack and a Mach number of 0.70 indicates that the axial-force coefficient of the glider with the advanced booster was approximately 22 percent higher than that of the glider with the original boosters. (See fig. 10.) The increased drag of the glider with advanced booster configuration would be expected since this configuration had nearly 20 percent more surface area than the glider with original boosters. The horizontal booster fins $\left(F_1\right)$ increased the drag of the glider and original boosters about 22 percent over the present Mach number range; whereas, the drag of the glider and original boosters was increased from 30 to 50 percent by the addition of the interdigitated booster fins $\left(F_2\right)$.

Pitching-moment characteristics.- The glider with original boosters and the glider with advanced boosters were longitudinally unstable as indicated by the positive values of the pitching-moment-curve slope C_{m_α} shown in figure 10. The position of the center of gravity of the model with respect to the moment reference axis of the present tests is not known; however, although stable values of the pitching-moment-curve slope were indicated for the glider with original boosters and interdigitated fins $\left(GB_{2T}B_{1T}F_2\right)$, it is believed that because of the small negative values of C_{m_α}, this configuration also would be longitudinally unstable. Because of the larger negative values of C_{m_α} indicated for configurations $GB_{2T}B_{1T}F_1$ and $NB_{2T}B_{1T}F_1$, these configurations may possibly be longitudinally stable. Because of the variations of the pitching-moment-curve slope C_{m_α} and the normal-force-curve slope C_{N_α}

with Mach number, all the configurations experienced only a small shift
of the center-of-pressure location throughout the speed range of the
present tests.

Elevon effectiveness.- The value of the elevon control effective-
ness parameter $C_{m_{\delta_e}}$ for the glider with the original boosters was low
and decreased approximately 50 percent as Mach number increased from
about 0.90 to 1.20. (See fig. 11.) The elevon control effectiveness
parameter of the configuration was greatly increased by the addition of
the interdigitated booster fins (F_2). This parameter was still further
increased for the configuration with the horizontal booster fins (F_1)
so that at subsonic Mach numbers, the elevon control effectiveness was
approximately 4.5 times the value noted for the configuration without
booster fins.

Lateral Aerodynamic Characteristics

The basic static lateral aerodynamic characteristics for the various
model configurations are presented in figures 12 to 16 and are summarized
in figure 17.

It will be noted that there were some variations in the lateral
aerodynamic coefficients with angle of attack at zero angle of sideslip.
These variations were particularly noticeable in the yawing-moment char-
acteristics for the configurations with the booster fins on. (See
figs. 6, 7, and 9.) Although there is no apparent reason for the varia-
tions in the lateral aerodynamic characteristics, it is believed that
some of these variations could be due in part to asymmetry of the model.

Directional stability characteristics.- For $\beta \approx 5^O$, elevon deflec-
tion caused the yawing-moment coefficients of the glider and original
boosters with and without the horizontal booster fins (fig. 12) to vary
in an erratic and inconsistent manner with angle of attack. Thus, a
comparison of figures 5 and 6 with figure 12 indicates that the con-
figurations could be either directionally stable or unstable, depending
upon elevon deflection and angle of attack.

In general, most of the configurations indicated positive direc-
tional stability (that is, positive values of the yawing-moment deriva-
tive C_{n_β}) throughout the Mach number range of the present tests at an
angle of attack of 0° (fig. 17(a)). Although a knowledge of the center-
of-gravity location for the launch configuration is not known, as was
previously mentioned, it is believed, with the possible exception of
configuration $GB_{2T}B_{1T}F_2$, that the various model configurations would
be aerodynamically unstable because of the very low measured positive

values of C_{n_β}. At an angle of attack of 5° (fig. 17(b)), the glider configuration with original boosters and the glider configuration with original boosters and horizontal booster fins were directionally unstable, as indicated by the negative values of C_{n_β}, whereas configuration $GB_{2T}B_{1T}F_2$ still had positive directional stability.

The side-force derivative C_{Y_β} for the various model configurations was only slightly affected by changes in angle of attack or by changes in Mach number (fig. 17). It will be noted that the configuration with the interdigitated booster fins F_2 caused an incremental increase in C_{Y_β} of approximately 0.02 throughout the Mach number range.

Effective dihedral.- At an angle of sideslip of 5°, the glider configuration with original boosters and horizontal booster fins experienced large variations of rolling-moment coefficient with angle of attack (fig. 12). These large variations in rolling-moment coefficient are obviously due to the negative geometric dihedral at low angles of attack and to the positive geometric dihedral at high angles of attack contributed by the horizontal booster-fin sweep since similar trends were not observed for the configuration without the horizontal booster fins. With the exception of configuration $GB_{2T}B_{1T}F_1$ at an angle of attack of 5°, most of the configurations indicated negative effective dihedral as the Mach number was increased to 1.20 (fig. 17).

SUMMARY OF RESULTS

The results of a wind-tunnel investigation at transonic speeds to determine the static longitudinal and lateral aerodynamic characteristics of a proposed hypersonic glider with several booster configurations are summarized as follows:

1. The only configurations that may have satisfactorily longitudinal stability characteristics were those with the horizontal booster fins.

2. The glider configuration with original boosters and interdigitated booster fins was the only configuration which may have favorable directional stability characteristics.

3. Most of the configurations indicated negative effective dihedral as the Mach number was increased to 1.20.

Langley Research Center,
        National Aeronautics and Space Administration,
            Langley Field, Va., July 13, 1960.

REFERENCES

1. Watts, Anna Belle: Basic Pressure Measurements at Transonic Speeds
        on Booster Configurations for a Proposed Hypersonic Glider. NASA
        TM X-225, 1960.

2. Braslow, Albert L., and Knox, Eugene C.: Simplified Method for
        Determination of Critical Height of Distributed Roughness Particles
        for Boundary-Layer Transition at Mach Numbers From 0 to 5. NACA
        TN 4363, 1958.

3. Osborne, Robert S.: High-Speed Wind-Tunnel Investigation of the
        Longitudinal Stability and Control Characteristics of a 1/16-Scale
        Model of the D-558-2 Research Airplane at High Subsonic Mach Num-
        bers and at a Mach Number of 1.2. NACA RM L9C04, 1949.

Figure 1.- Glider details. All dimensions are in inches unless otherwise noted.
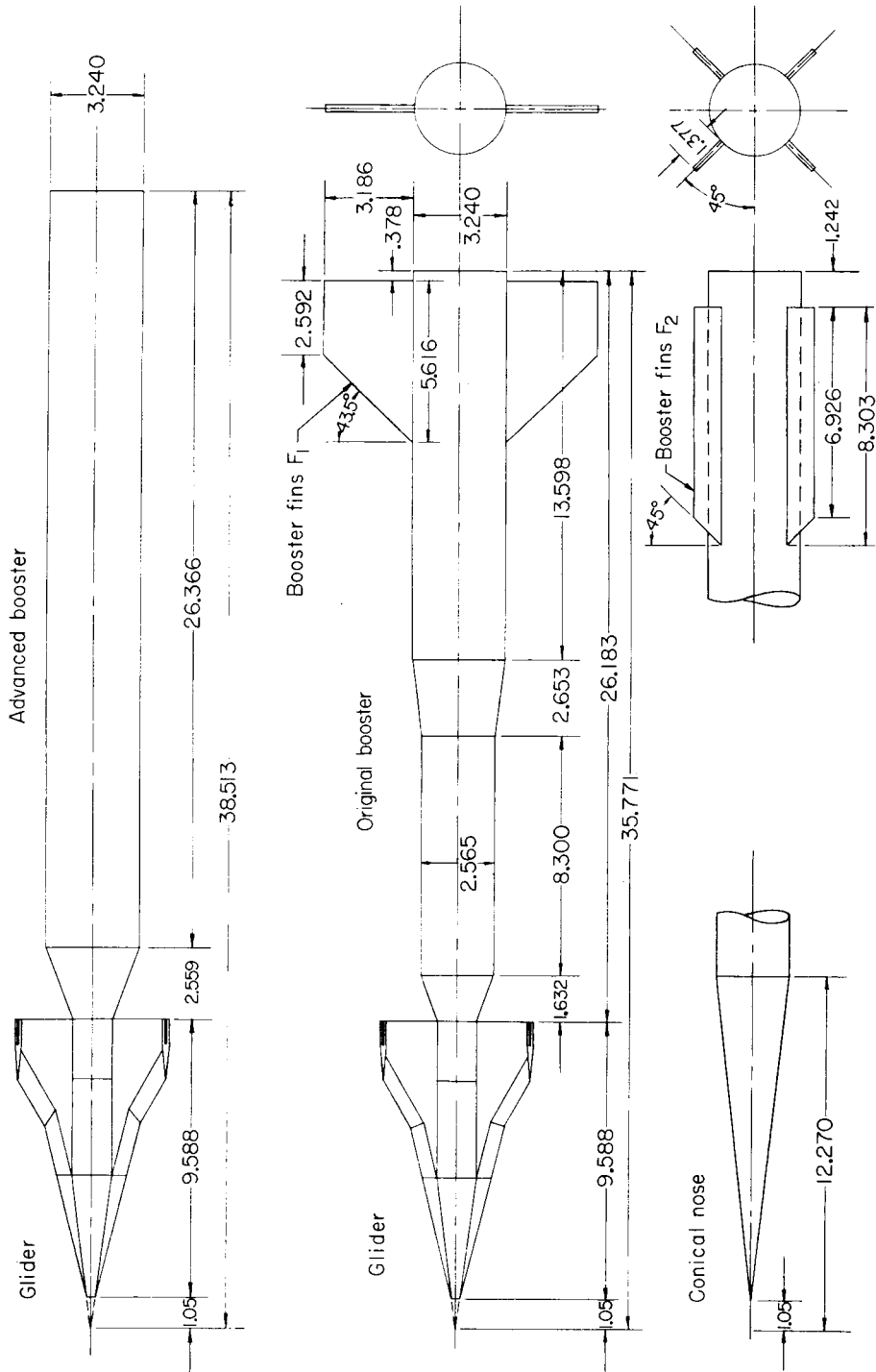
Figure 2.- Complete model details. All dimensions are in inches unless otherwise noted.

L-59-564
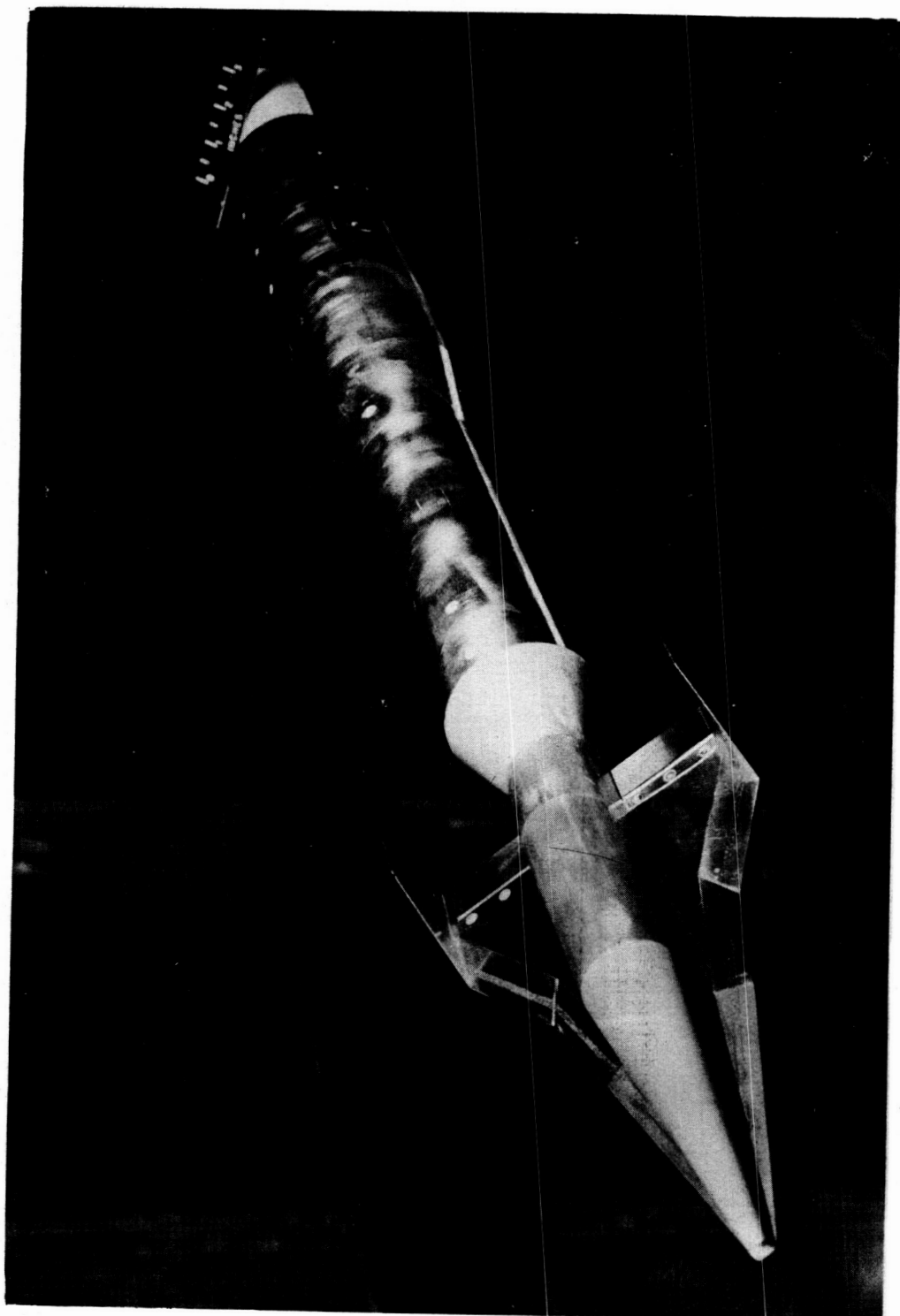
Figure 3.- Glider and original boosters mounted on sting support in Langley 8-foot transonic pressure tunnel.
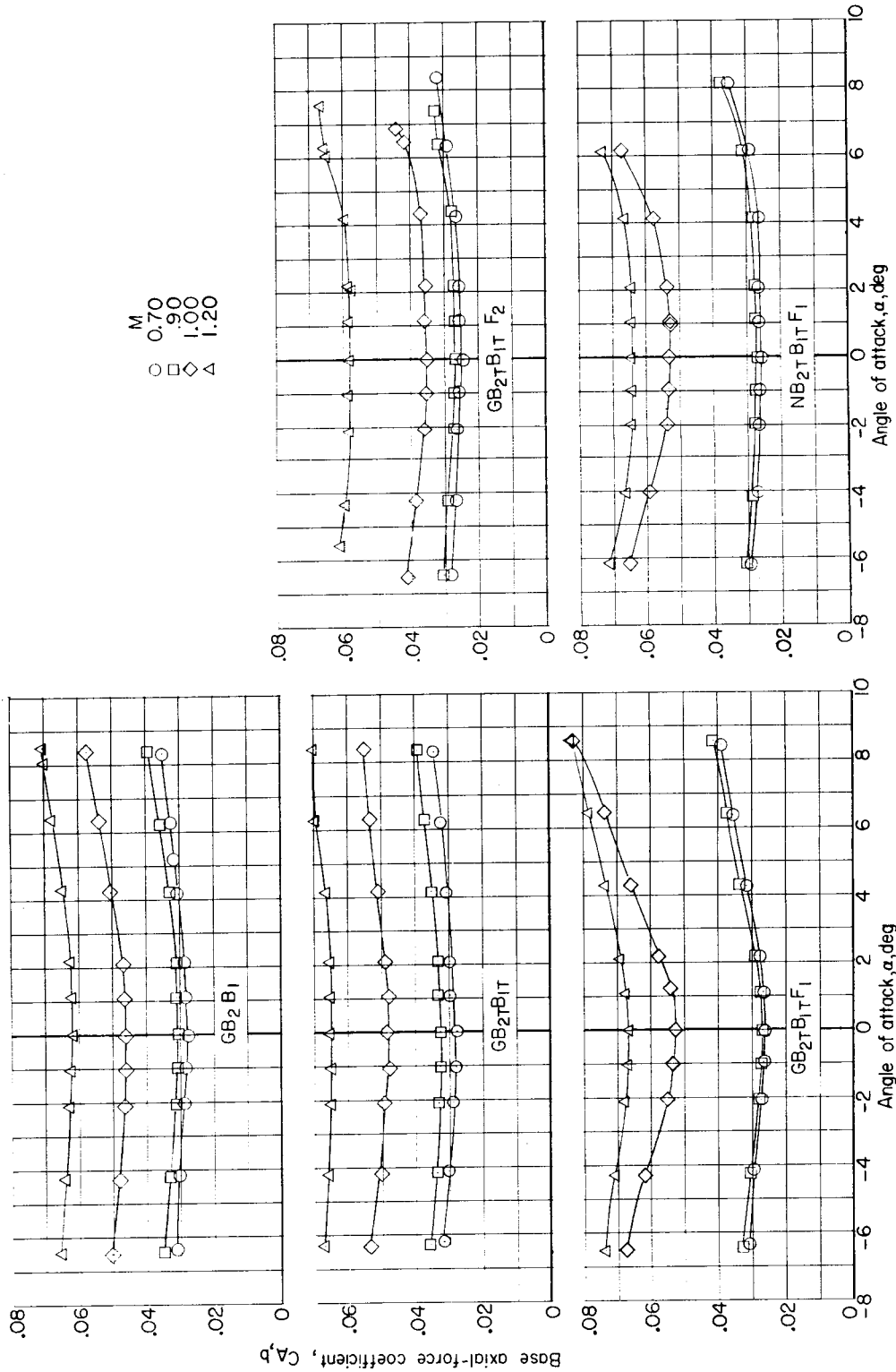
Figure 4.- Variations with angle of attack of the base axial-force coefficient for several configurations.
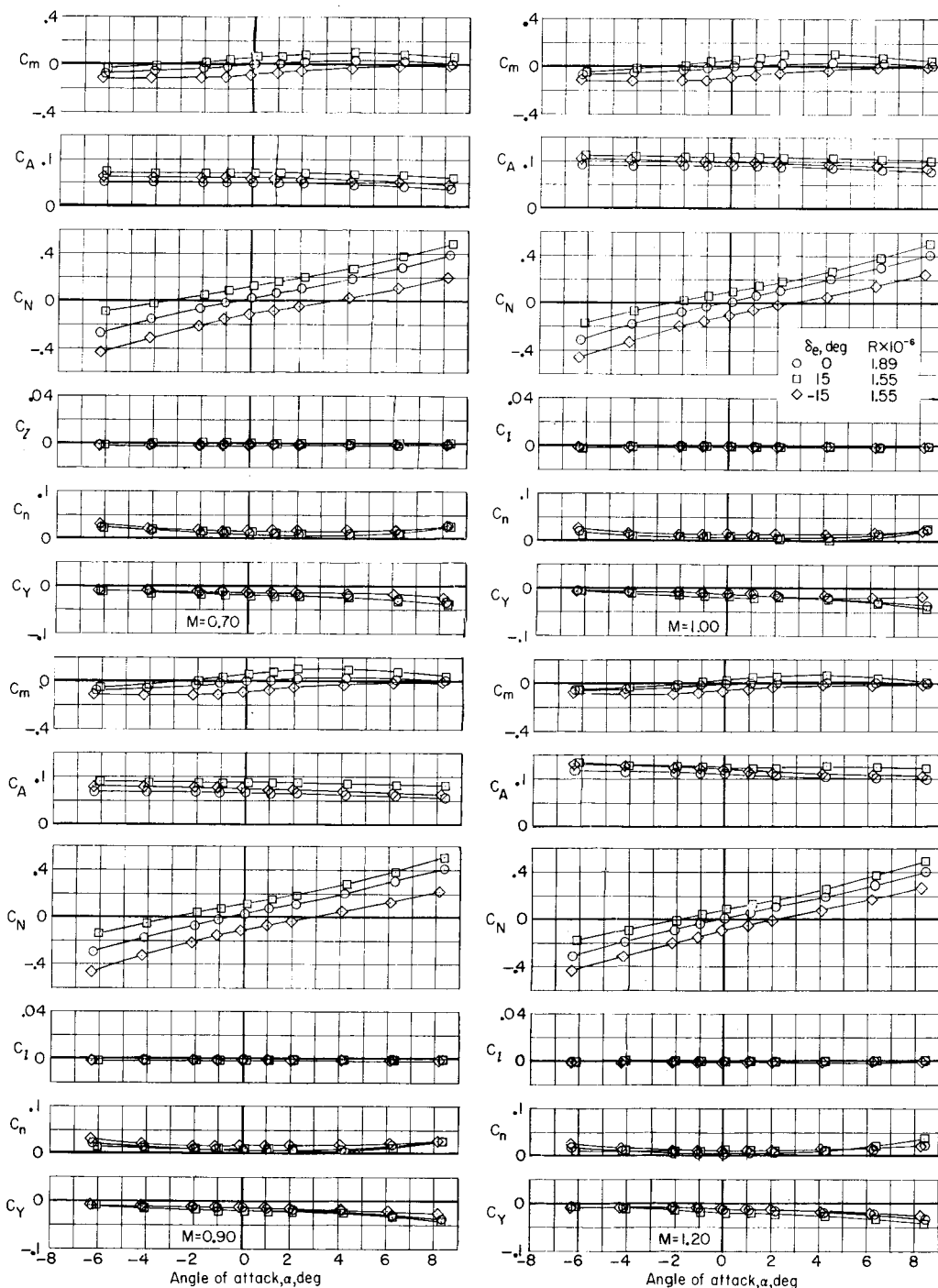
Figure 5.- Effect of elevon deflection on aerodynamic characteristics in pitch for the glider configuration with original boosters $\left(GB_{2T}B_{1T}\right)$.
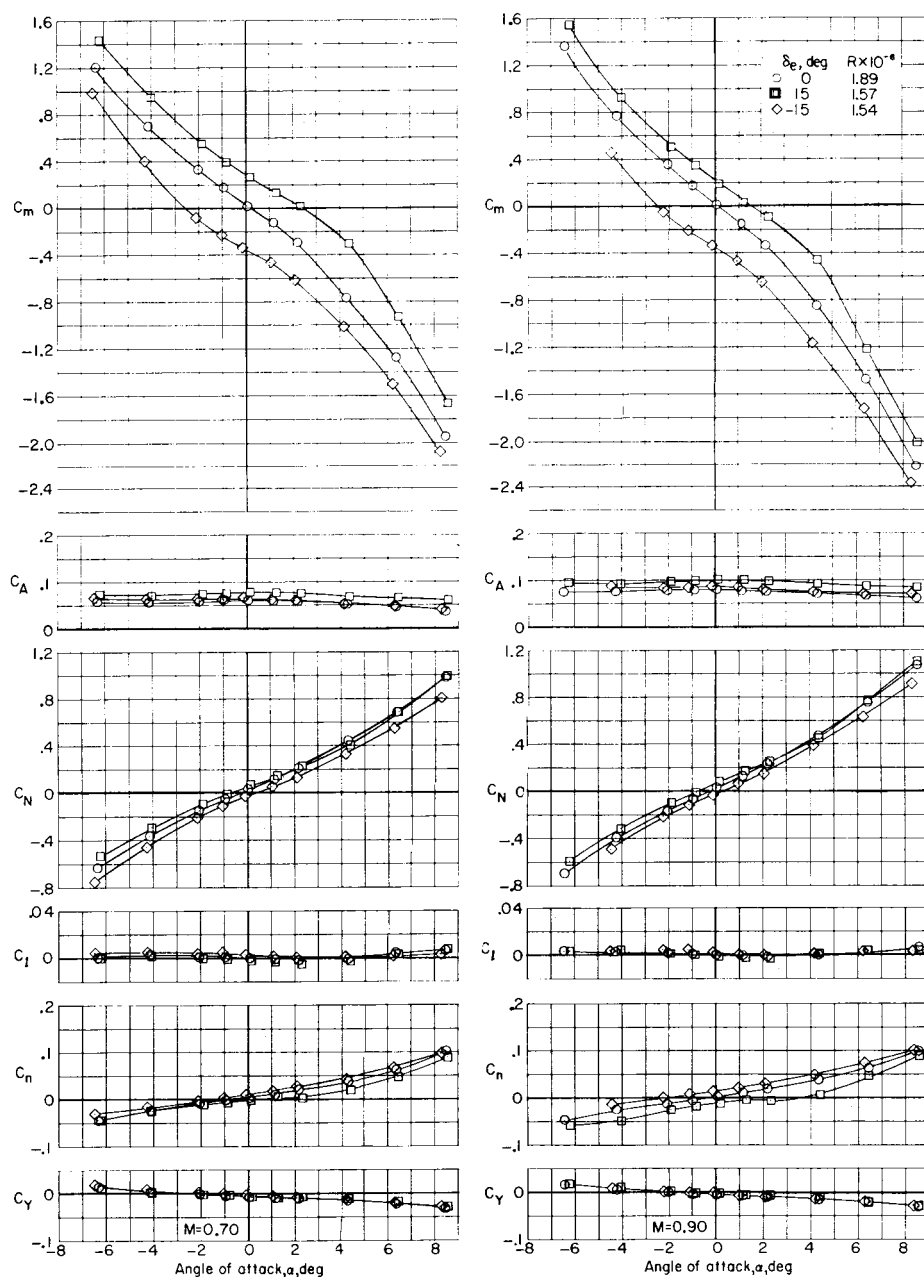
(a) M = 0.70 and 0.90.

Figure 6.- Effect of elevon deflection on aerodynamic characteristics in pitch for the glider configuration with original boosters and horizontal booster fins $\left(GB_{2T}B_{1T}F_1\right)$.
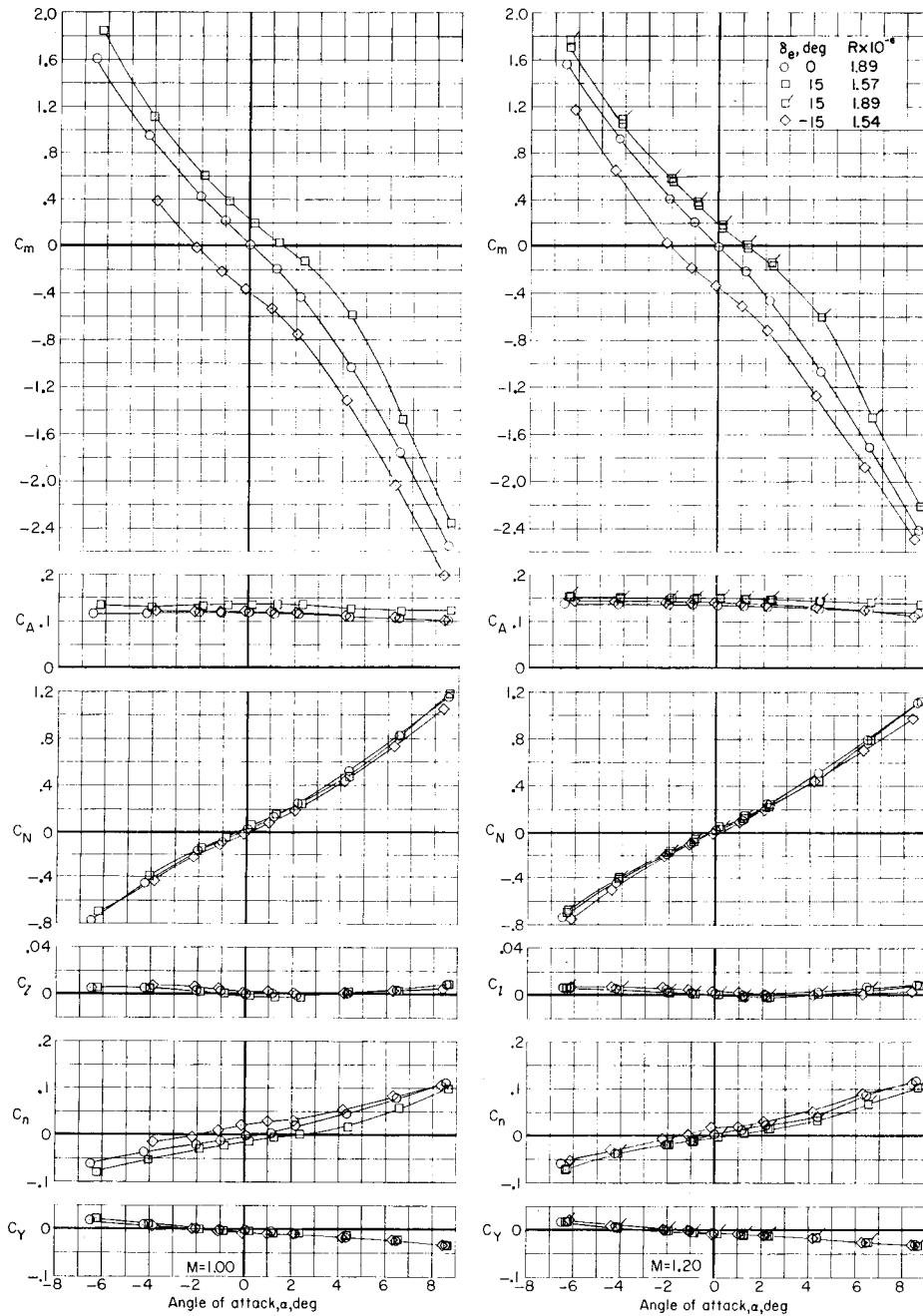
(b) M = 1.00 and 1.20.

Figure 6.- Concluded.

CONFIDENTIAL
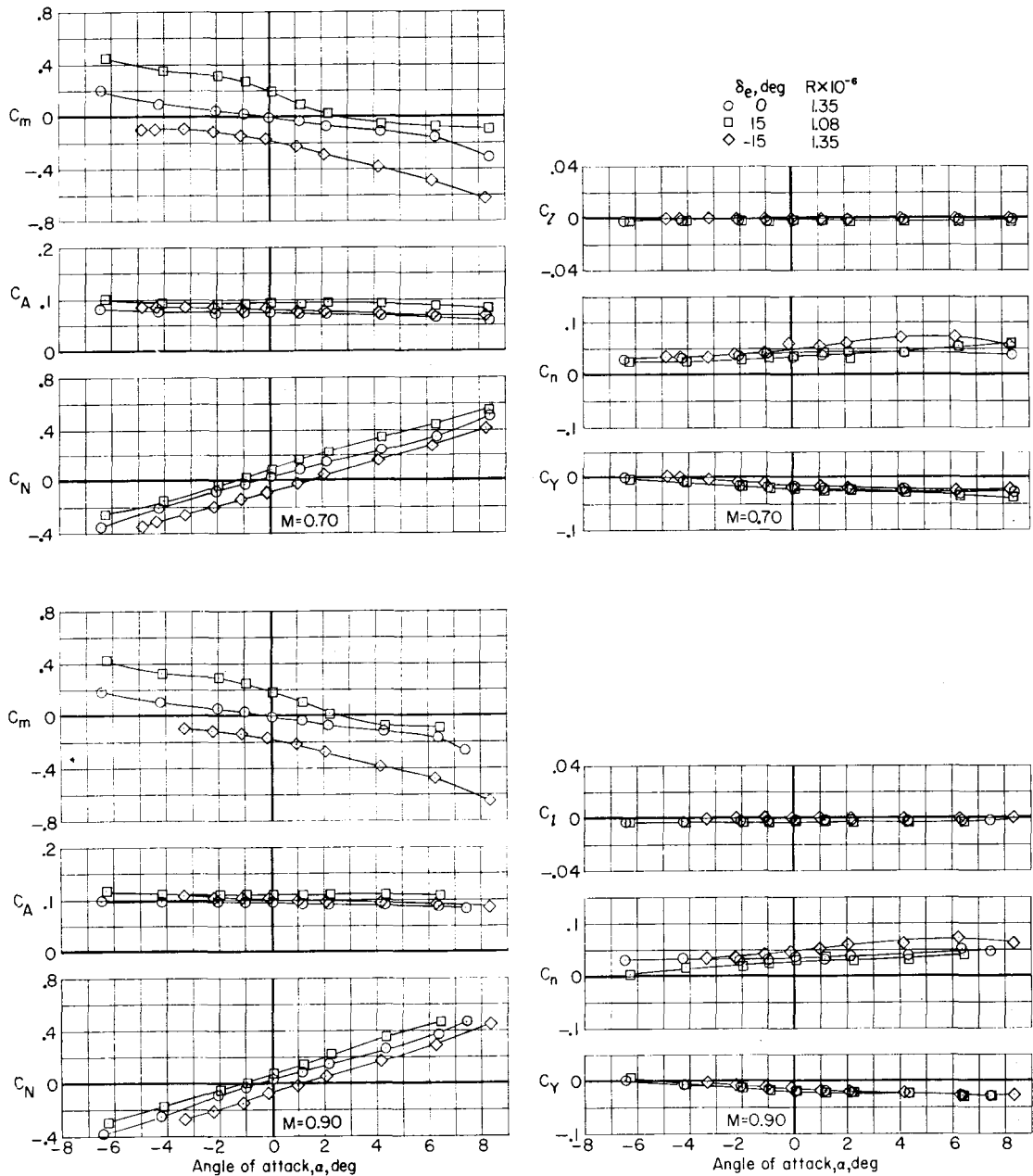
(a)   M = 0.70 and 0.90.

Figure 7.- Effect of elevon deflection on aerodynamic characteristics in
    pitch for the glider configuration with original boosters and inter-
    digitated booster fins $\left(GB_{2T}B_{1T}F_2\right)$.
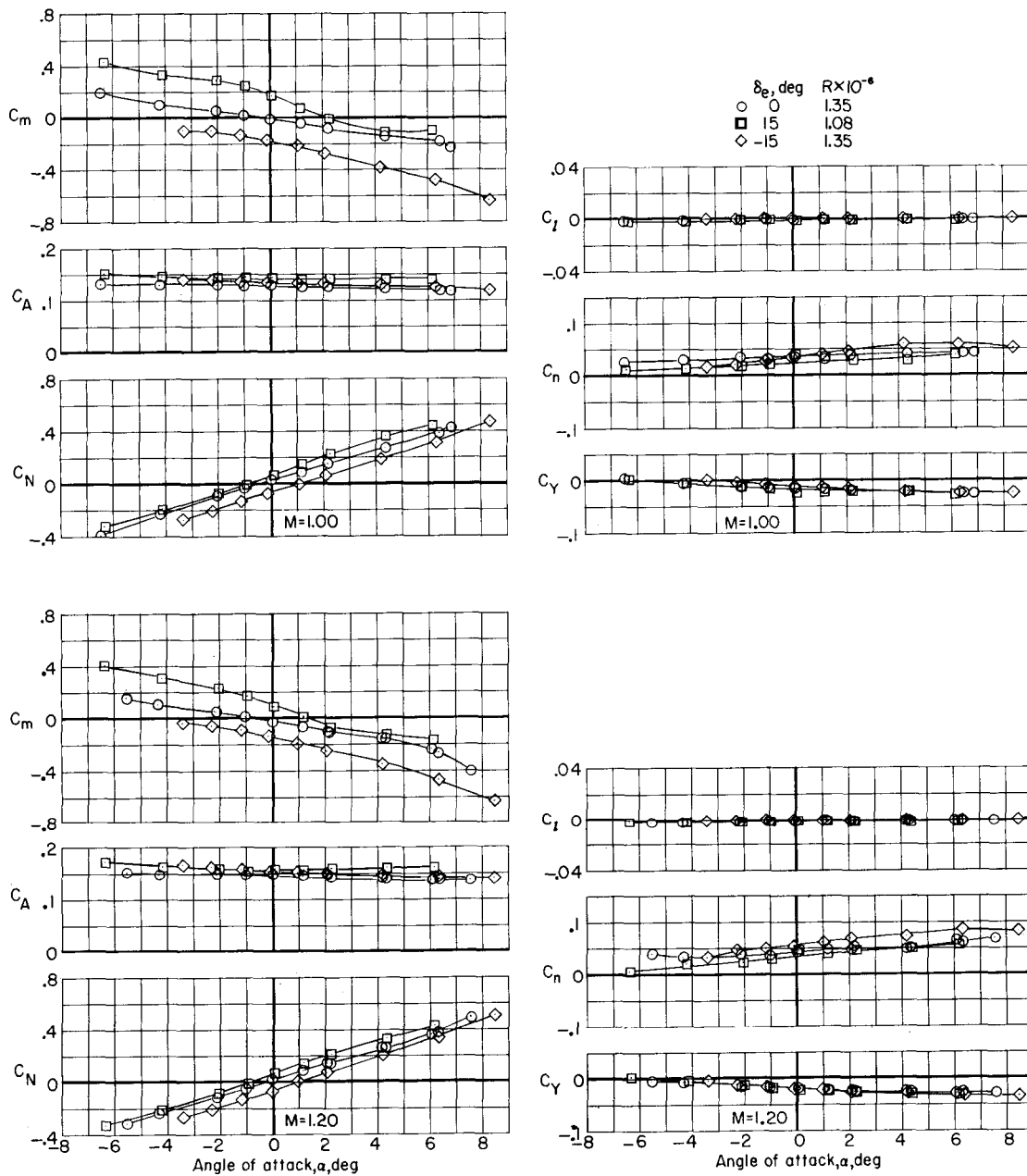
(b)   M = 1.00 and 1.20.

Figure 7.- Concluded.

Figure 8.- Aerodynamic characteristics in pitch for the glider configuration with advanced boosters (GB_2B_1). $R = 1.89 \times 10^6$.
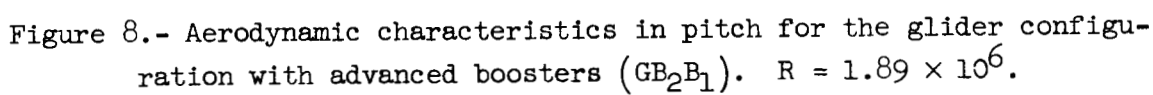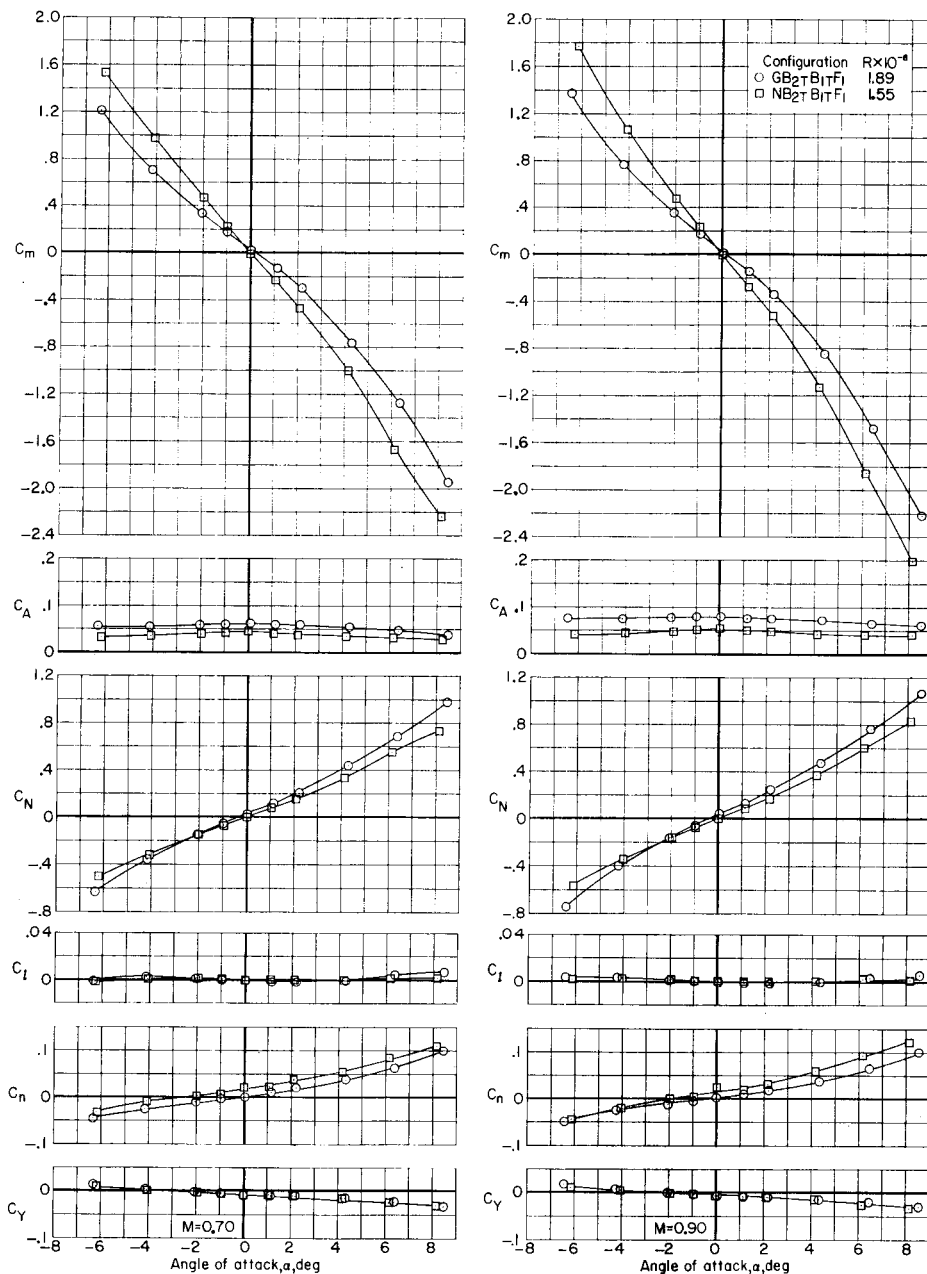
(a)   M = 0.70 and 0.90.

Figure 9.- A comparison of the aerodynamic characteristics in pitch of the glider and of the conical-nose configurations with the original boosters and horizontal booster fins.
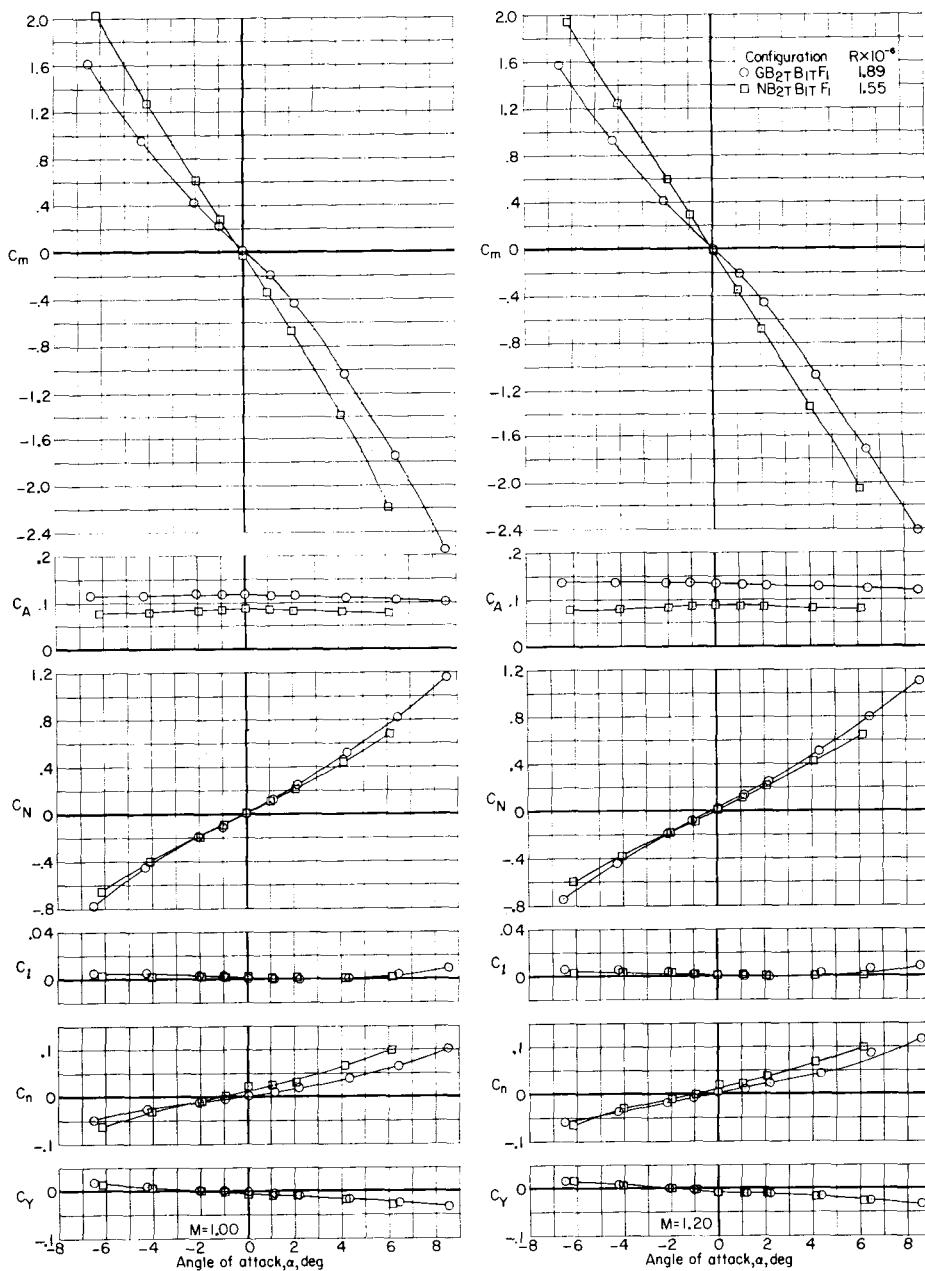
(b)   M = 1.00 and 1.20.

Figure 9.- Concluded.
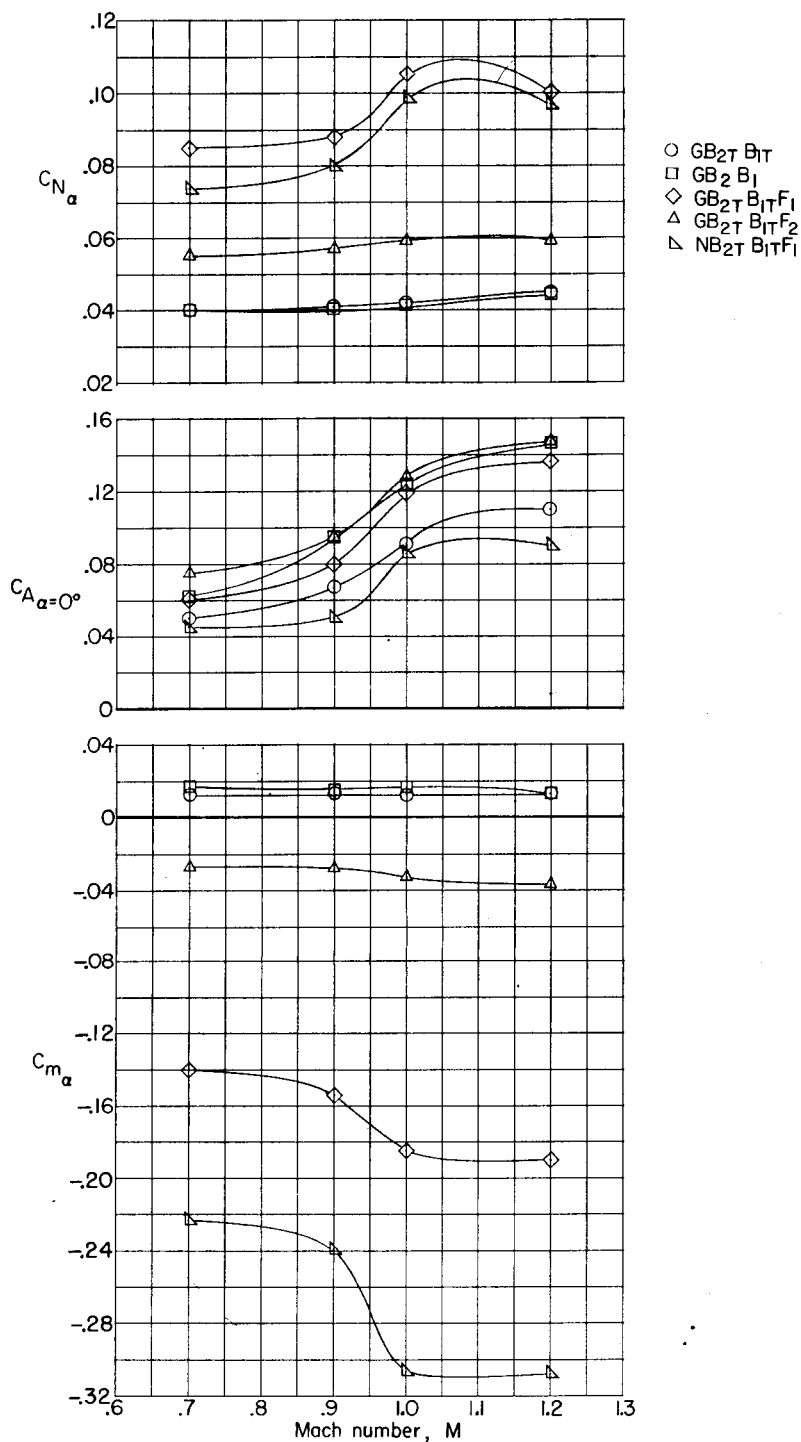
Figure 10.- Summary of the static longitudinal aerodynamic character-
istics of several model configurations.

Figure 11.- Variations with Mach number of elevon control effectiveness for the glider configuration with original boosters and with and without booster fins.
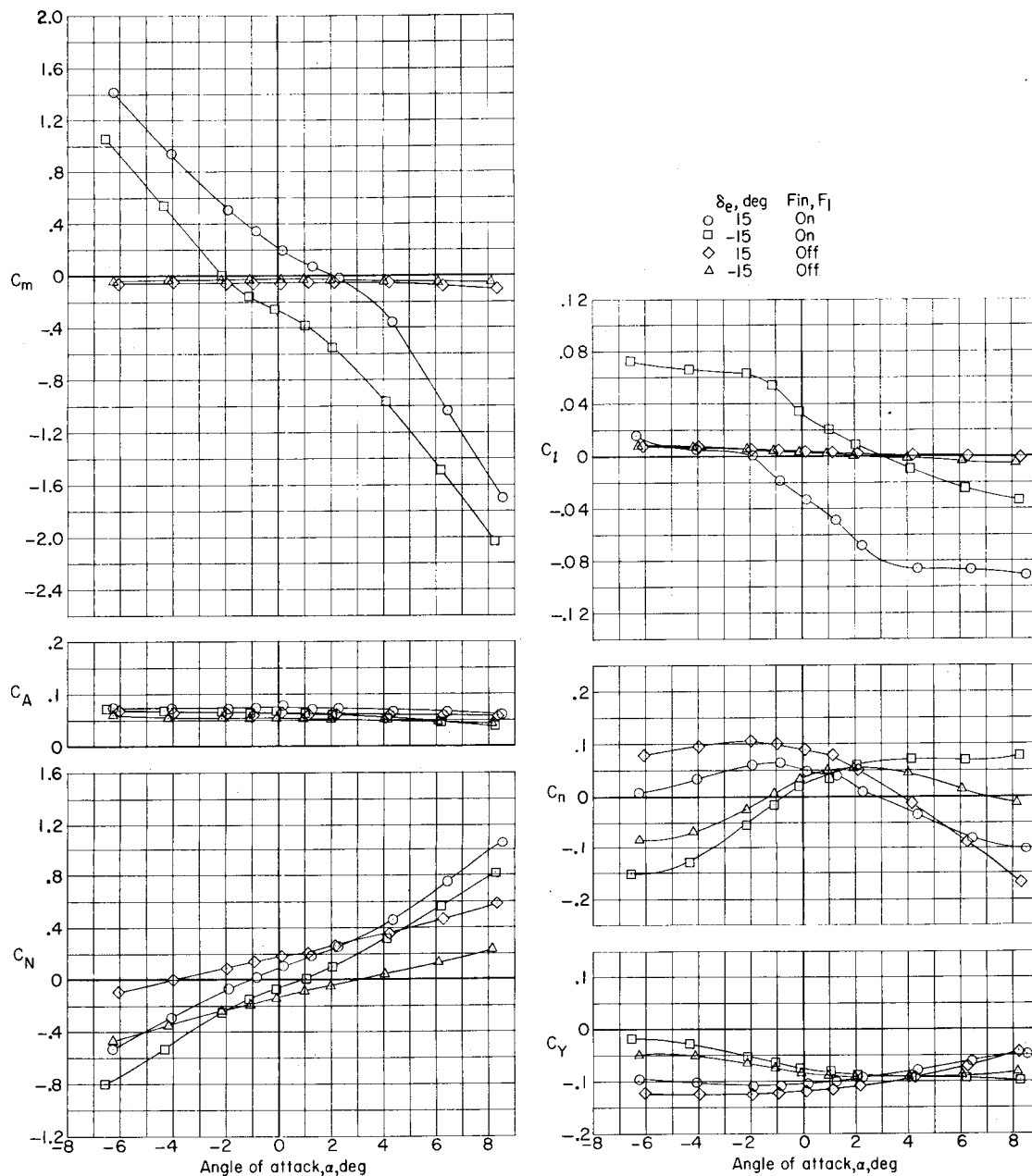
(a)   M = 0.70.

Figure 12.- Effect of elevon deflection on the aerodynamic character-
    istics in pitch of the glider configuration $GB_{2T}B_{1T}$ with and without
    horizontal booster fins. $\beta \approx 5°$; R = 1.55 × 10^6.

	δ_e, deg	Fin, F_1
○	15	On
□	-15	On
◇	15	Off
△	-15	Off

(b) M = 0.90.

Figure 12.- Continued.
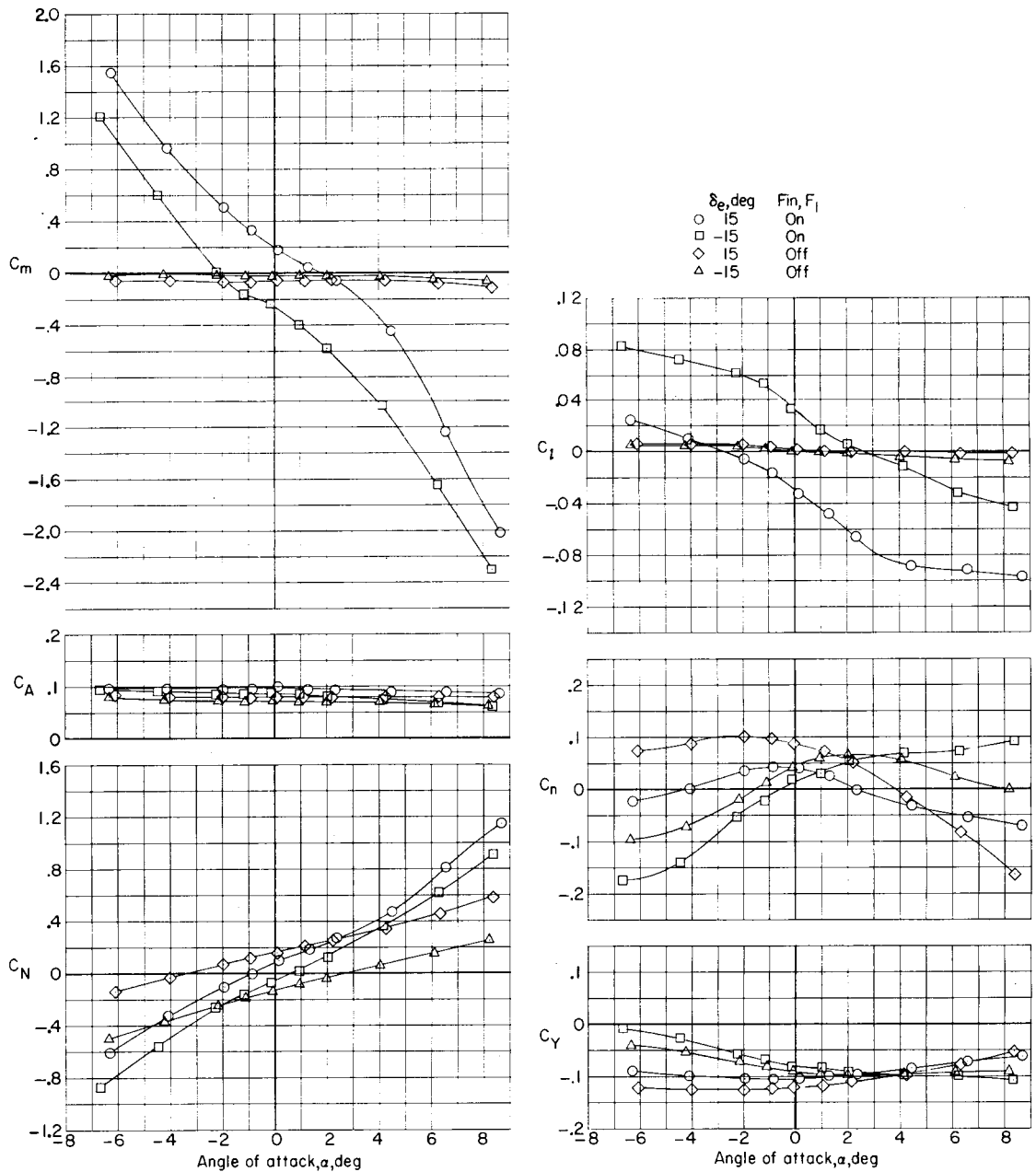
(c) M = 1.00.

Figure 12.- Continued.

CONFIDENTIAL
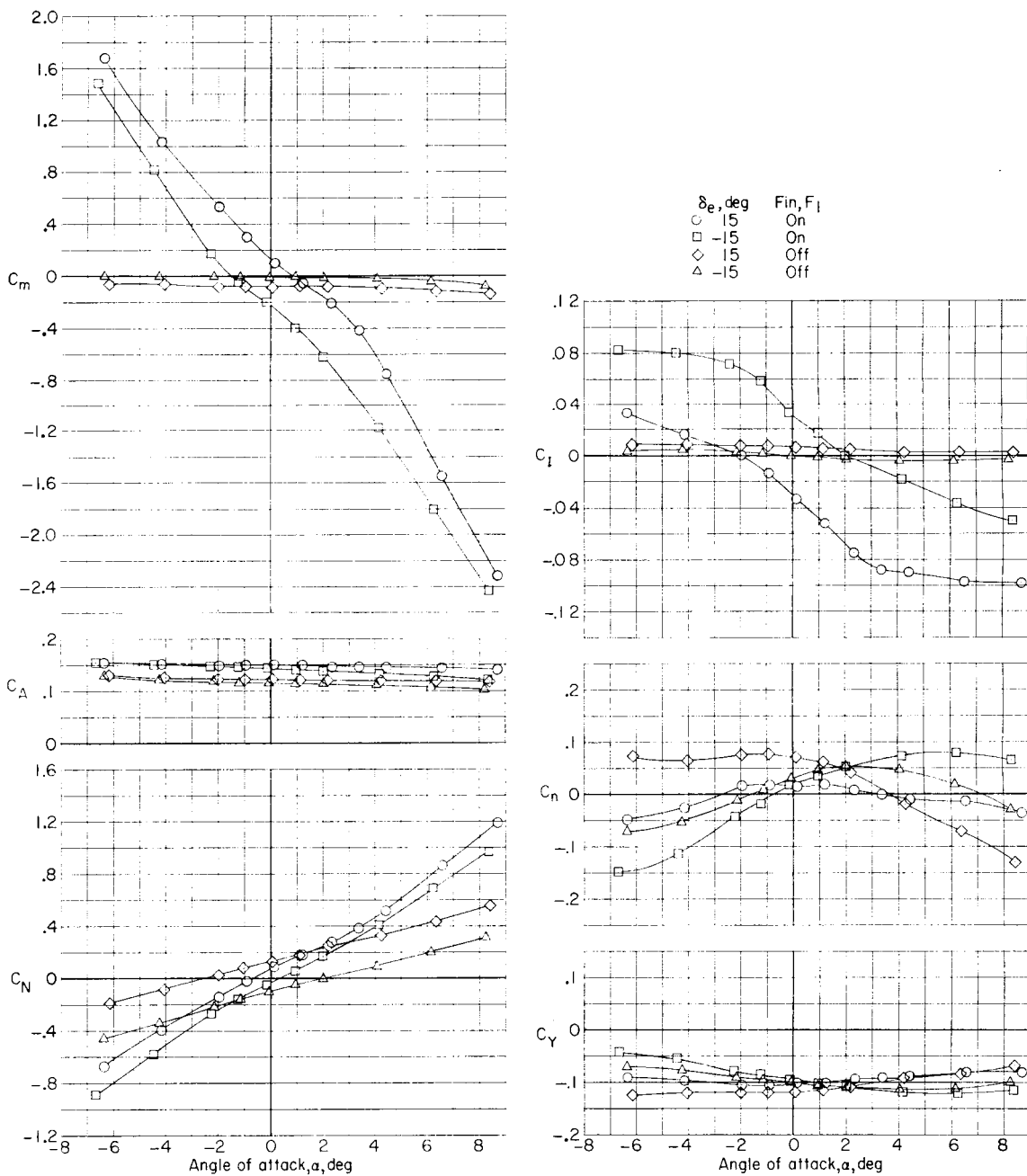
(d) M = 1.20.

Figure 12.- Concluded.

CONFIDENTIAL
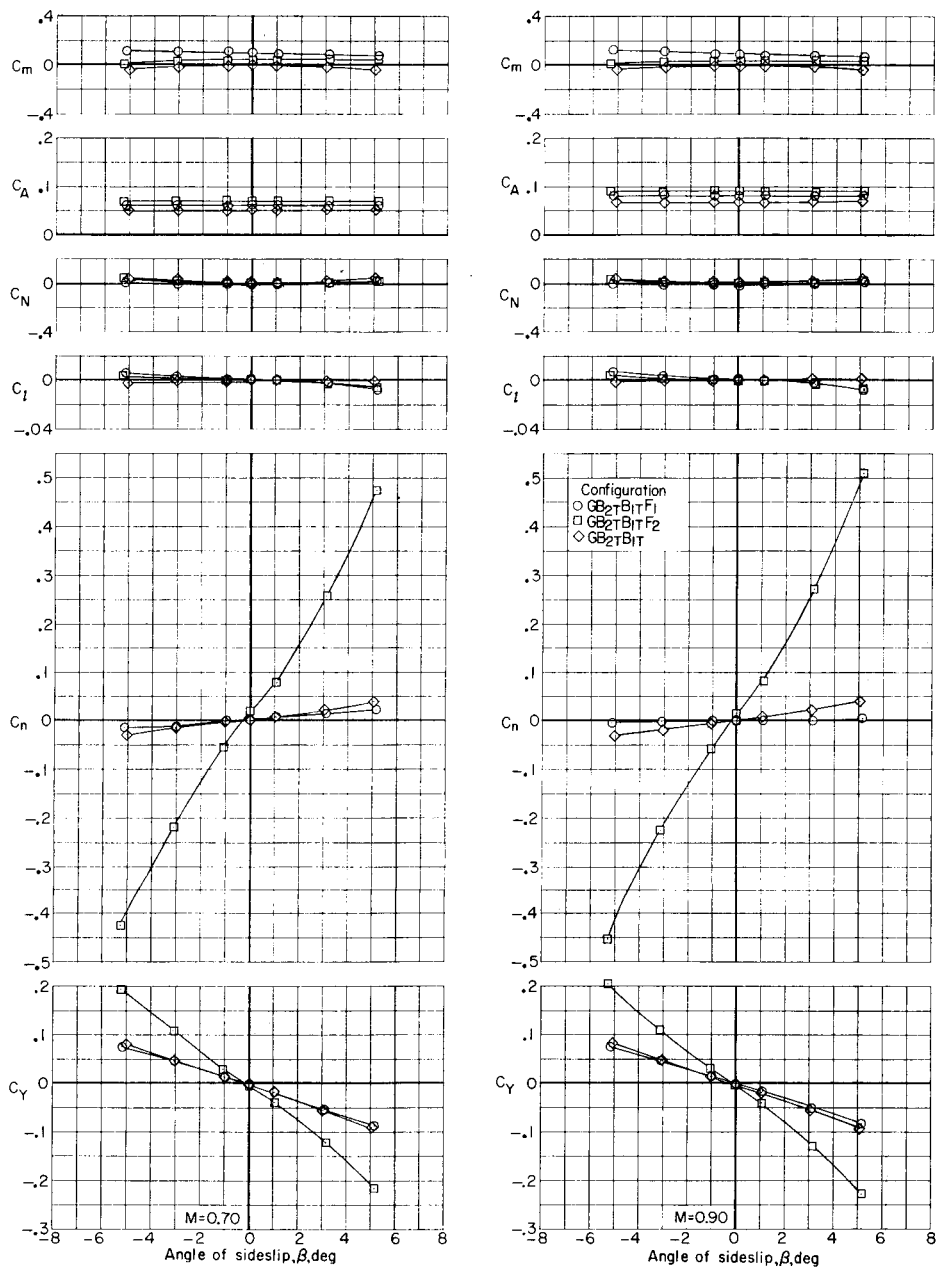
(a) M = 0.70 and 0.90.

Figure 13.- Aerodynamic characteristics in sideslip of the glider configuration with original boosters and with and without booster fins. $\alpha = 0^{o}$; $\delta_{e} = 0^{o}$; $R = 1.89 \times 10^{6}$.

CONFIDENTIAL
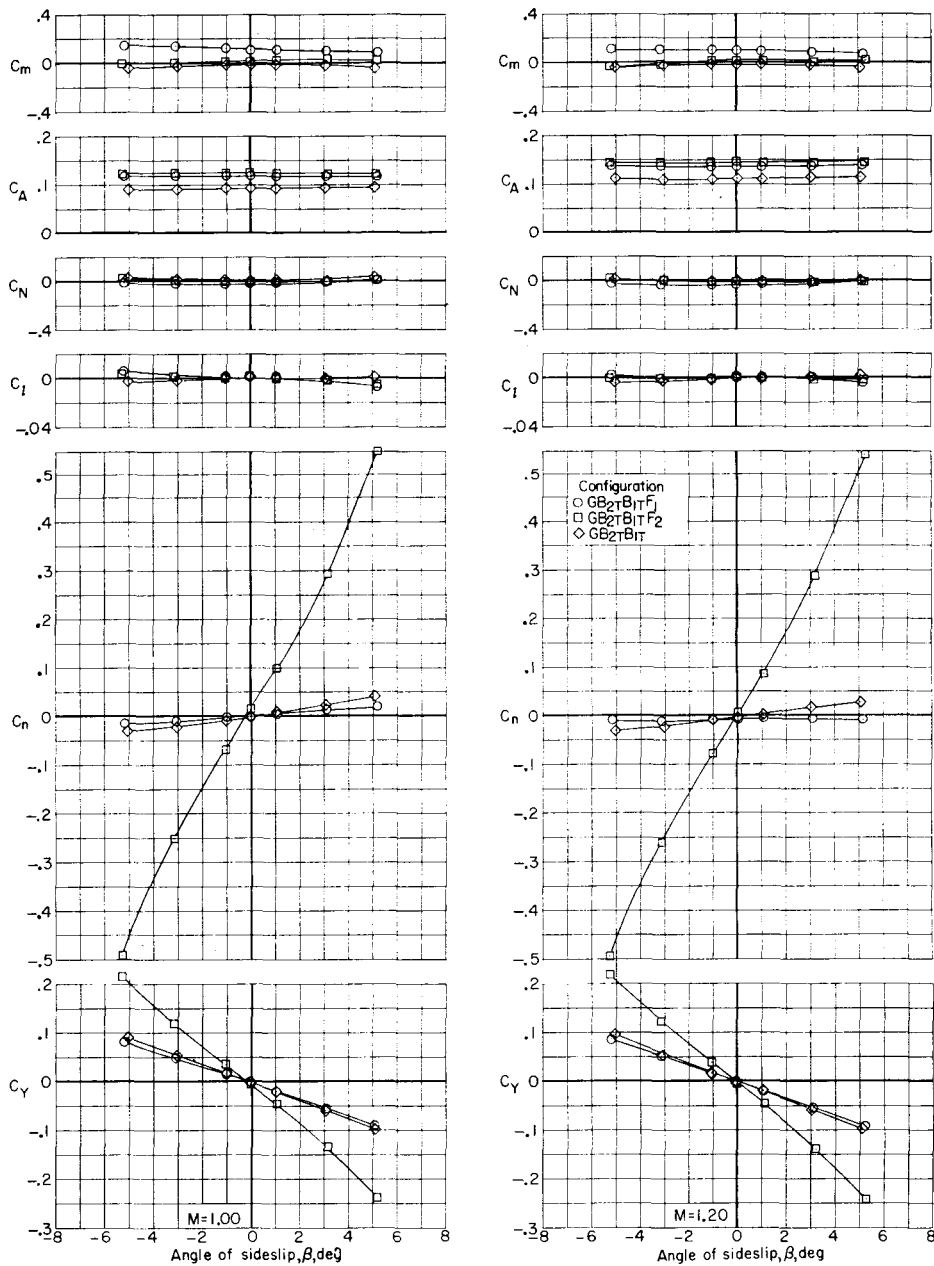
(b)   M = 1.00 and 1.20.

Figure 13.- Concluded.
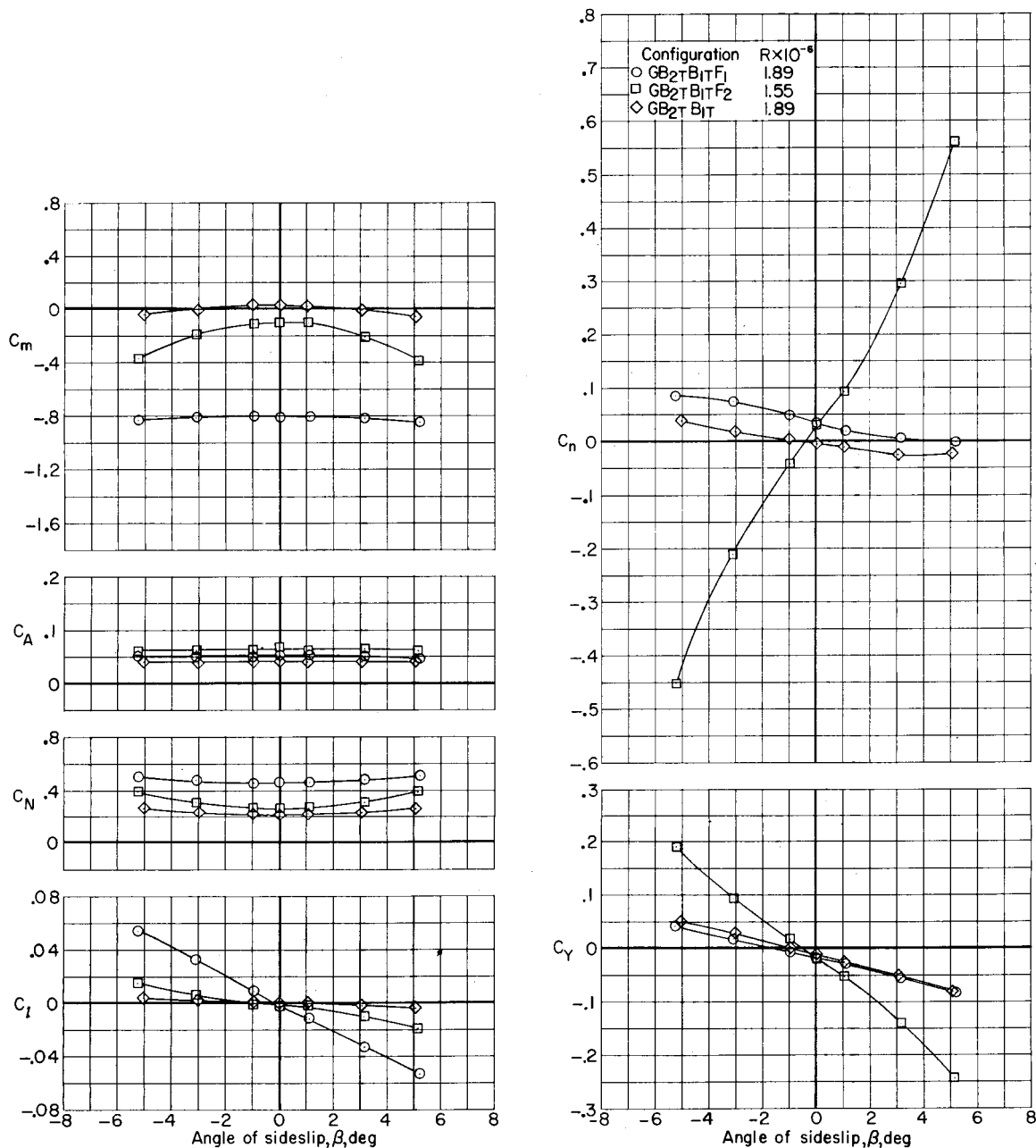
(a)   M = 0.70.

Figure 14.- Aerodynamic characteristics in sideslip of the glider con-
   figuration with original boosters and with and without booster fins.
   $\alpha \approx 5^{\circ}$; $\delta_e = 0^{\circ}$.
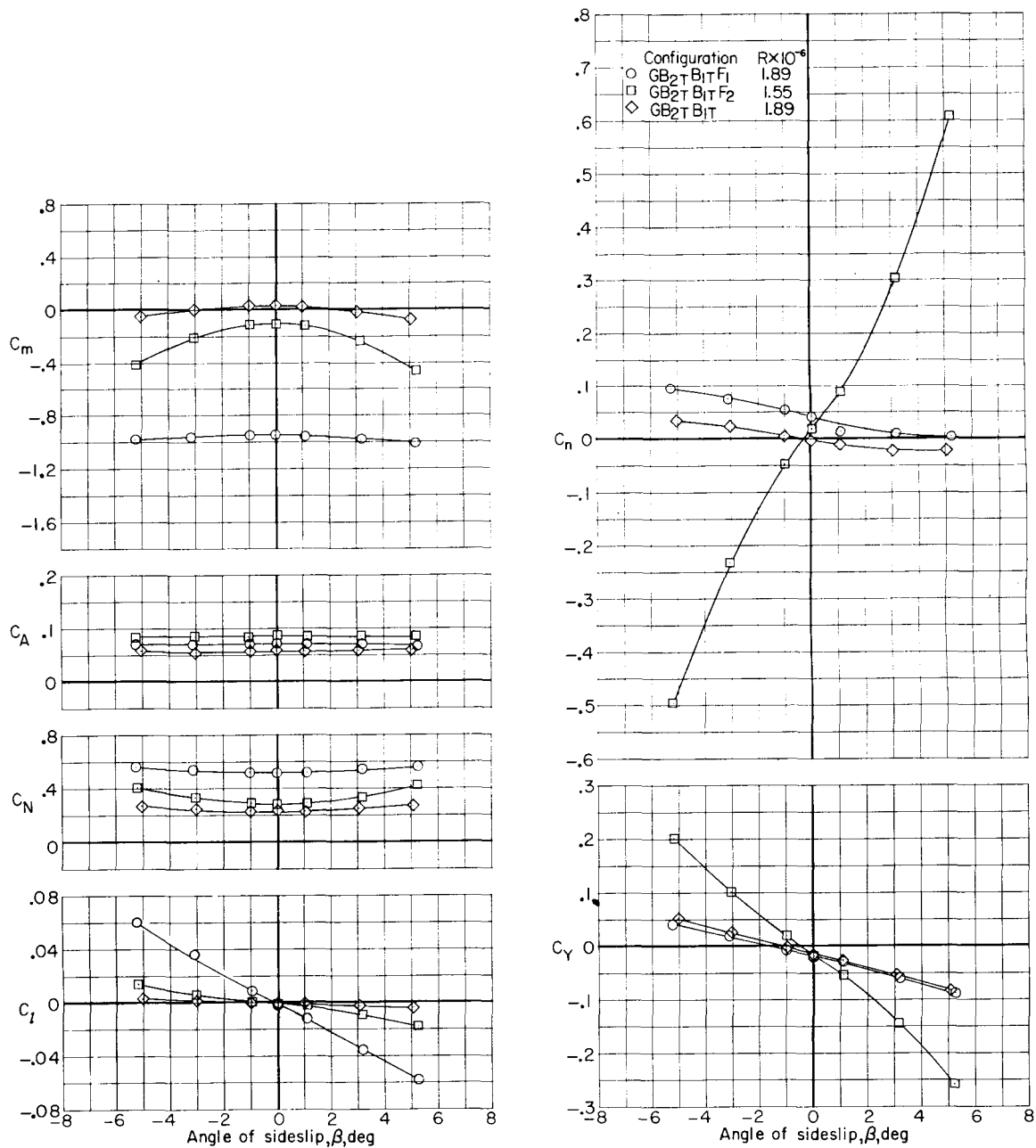
32   CONFIDENTIAL

(b)   M = 0.90.

Figure 14.- Continued.

(c) M = 1.00.

Figure 14.- Continued.
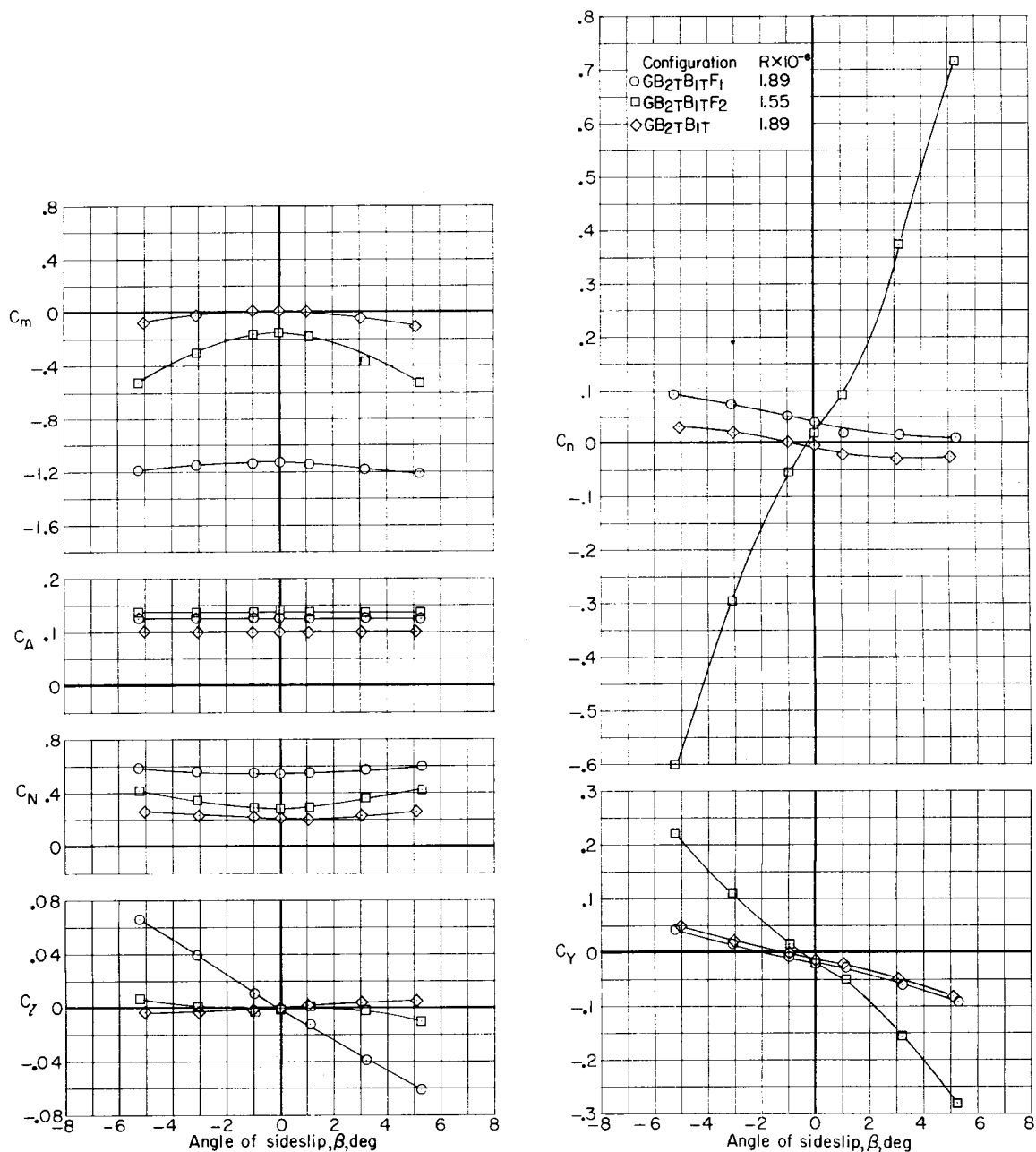
(d)   M = 1.20.

Figure 14.- Concluded.
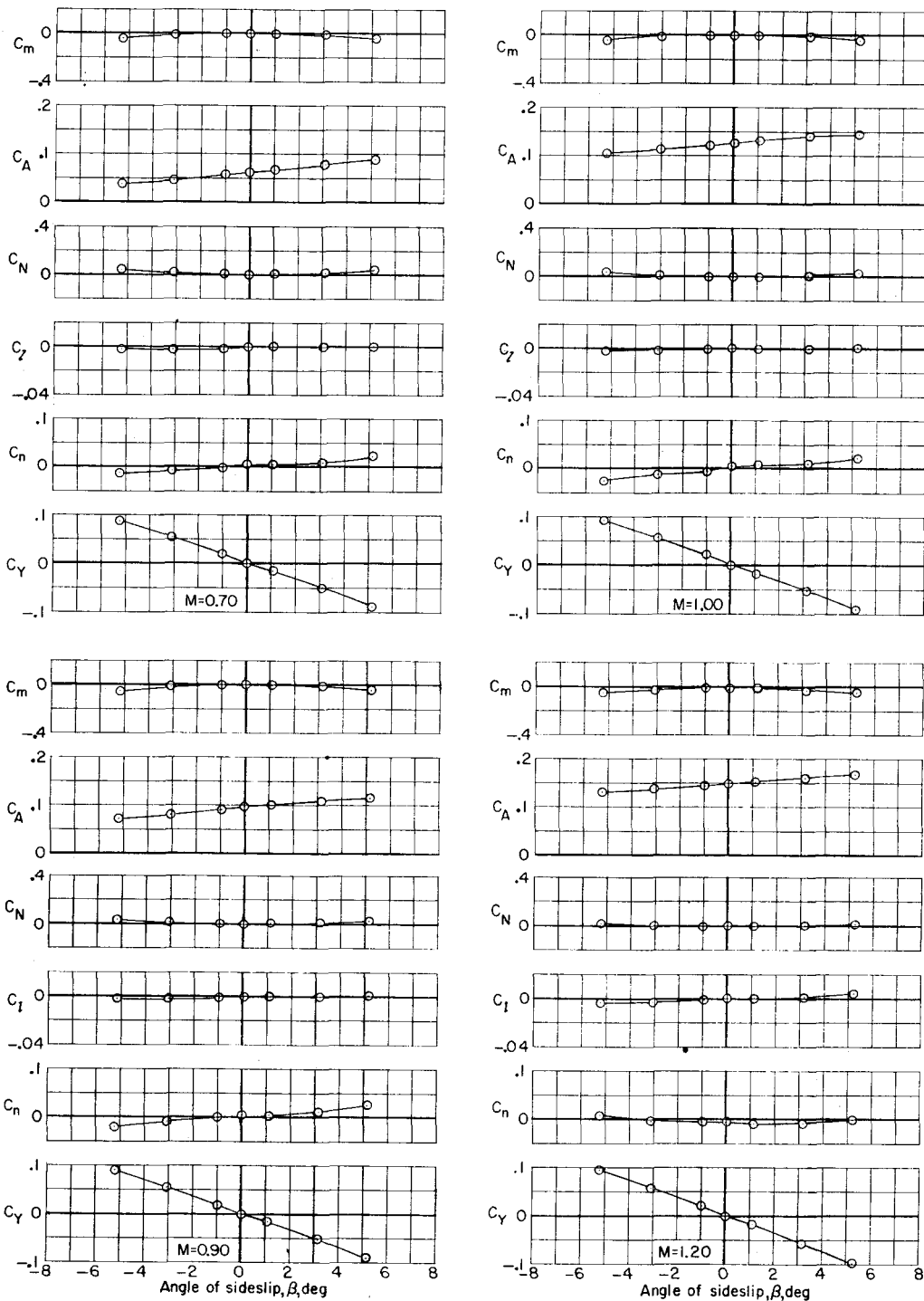
Figure 15.- Aerodynamic characteristics in sideslip of the glider configuration with advanced boosters. $\alpha = 0°$; $\delta_e = 0°$; $R = 1.89 \times 10^6$.
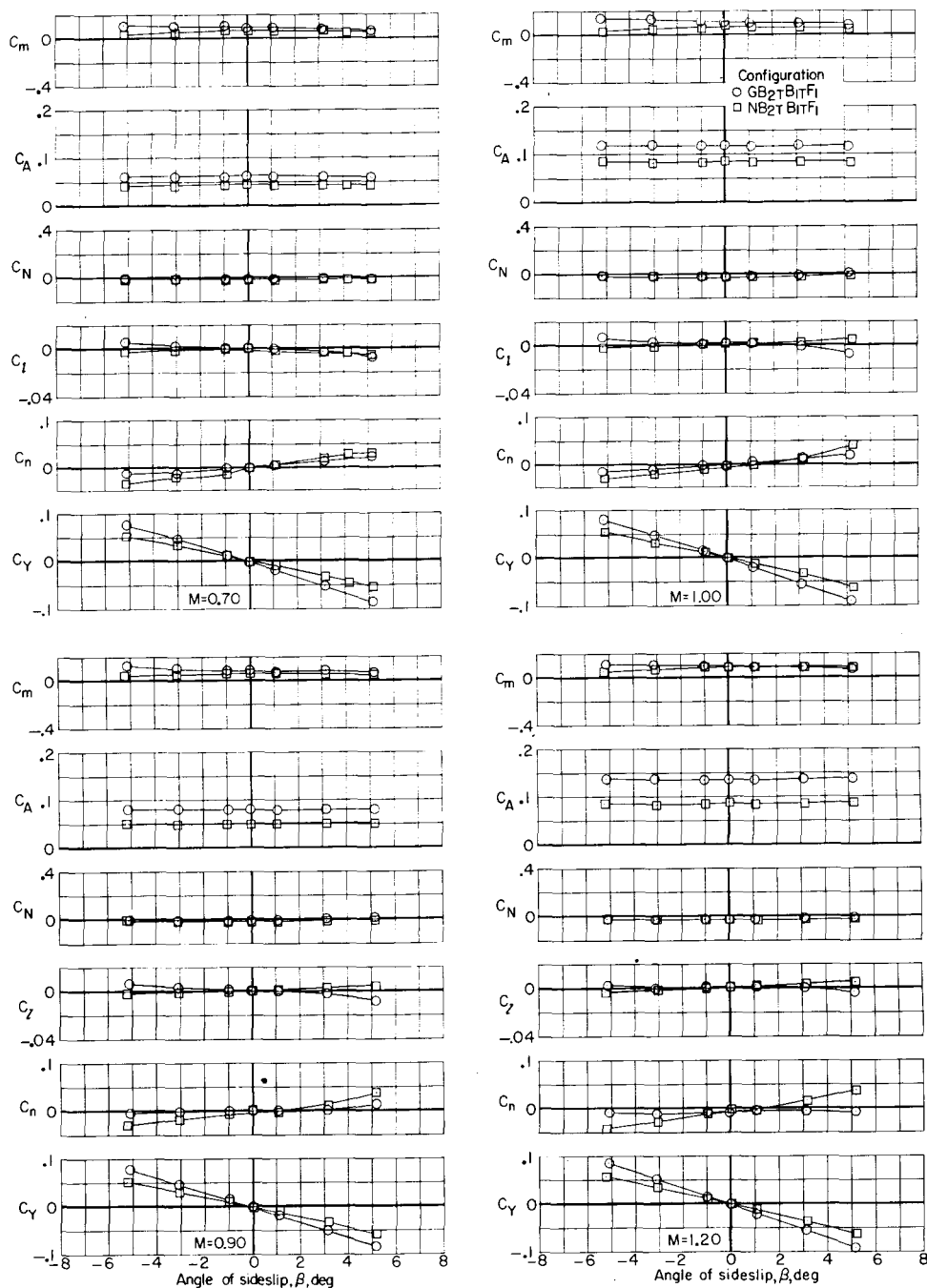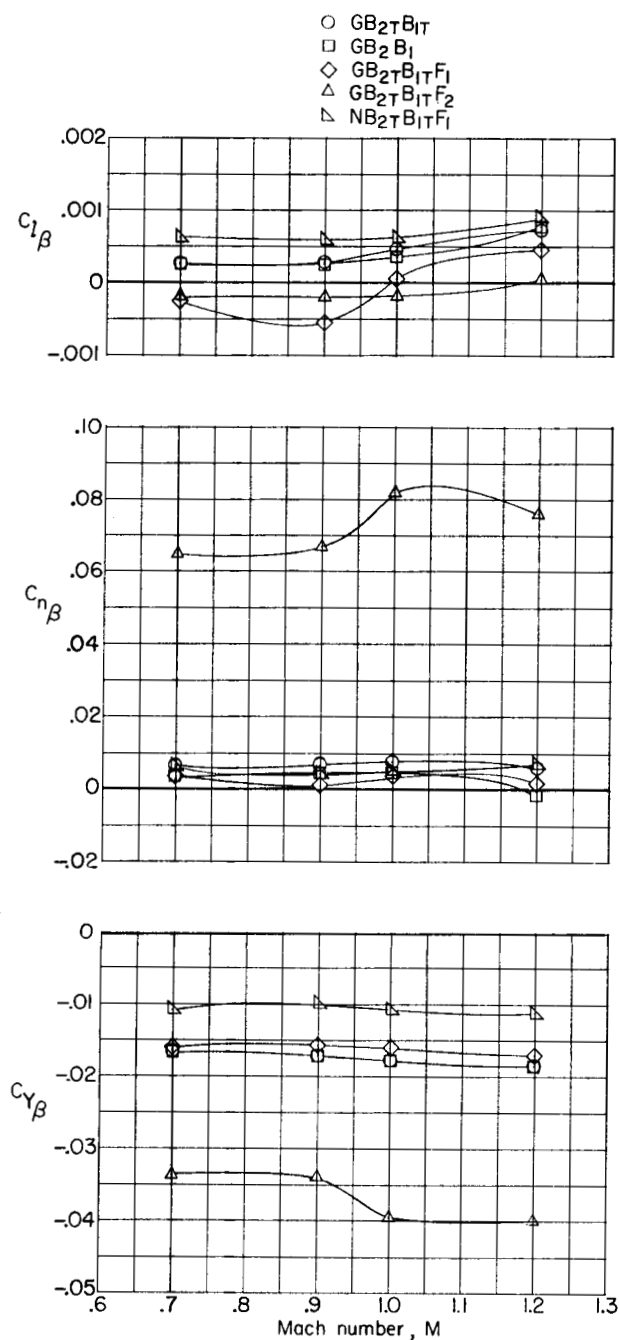
Figure 16.- A comparison of the aerodynamic characteristics in side-slip of the glider and of the conical-nose configurations with the original boosters and horizontal booster fins. $\alpha = 0^{\circ}$; $\delta_e = 0^{\circ}$; $R = 1.89 \times 10^6$.

(a) α = 0°.
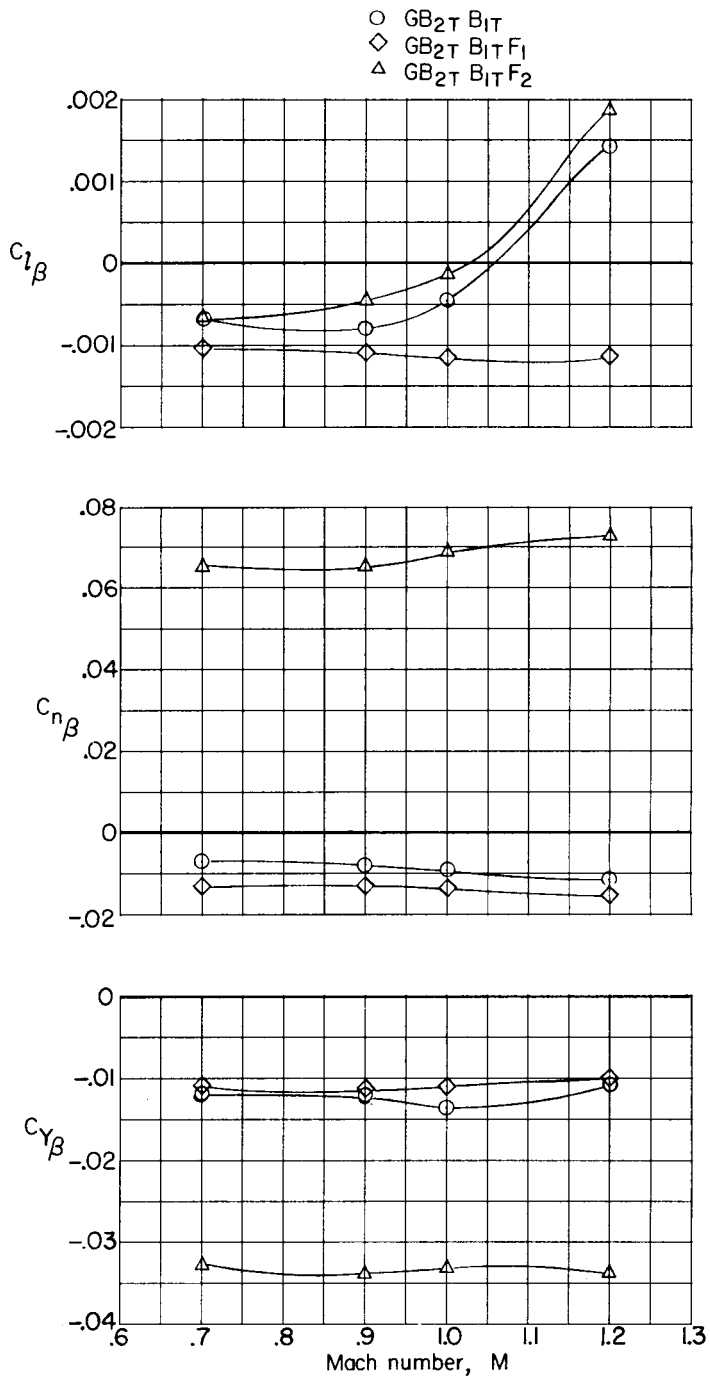
Figure 17.- Summary of the static-lateral-aerodynamic characteristics
of several model configurations.

CONFIDENTIAL

(b) $\alpha \approx 5^\circ$.

Figure 17.- Concluded.